PHYSICAL REVIEW A VOLUME 51, NUMBER 2 FEBRUARY 1995

Photoelectron statistics of solitons corrupted by amplified spontaneous emission

Takayuki Yoshino and Govind P. Agrawal
The Institute of Optics, University of Rochester, Rochester, New York 14627
(Received 30 August 1994)

The probability density function (PDF) of photoelectron counts is investigated theoretically for a fundamental soliton corrupted by the spontaneous-emission noise that is generated by optical amplifiers employed along a fiber-optic transmission line. An analysis based on the orthogonal expansion of the light amplitude makes it possible to find the exact PDF that includes the influence of the soliton width, the hyperbolic-secant pulse shape, and a Lorentzian bandpass optical filter. The derived PDF is applicable to any cascaded chain of amplifiers and, as a practical example, is calculated for a receiver equipped with an optical preamplifier. The pulse width significantly affects photoelectron statistics when the product of the filter bandwidth and the counting interval is small. By comparing our exact PDF with the commonly used approximate Gaussian and Laguerre PDFs, we find that such approximations introduce large errors (by several orders of magnitude) in the tail of the PDF that is relevant for calculation of bit error rates in soliton communication systems.

PACS number(s): 42.50.Ar, 42.50.Rh

I. INTRODUCTION

Soliton communication systems with optical amplifiers appear to be drawing increasing attention as a key technology useful for long-distance transmission at high bit rates [1]. The aim of this paper is to calculate the probability density function (PDF) for photoelectrons generated when solitons corrupted by the optical amplifier noise are detected.

Since spontaneous emission generally accompanies coherent amplification, the signal pulses are always accompanied by amplified spontaneous emission (ASE) when optical amplifiers are employed in a transmission line. Interferential intensity fluctuations induced by this mixture of the coherent and chaotic fields lead to a serious increase of bit error rates in communication systems. In particular, receiver performance of soliton communication systems, where relatively energetic signal pulses are detected (so that thermal noise is negligible), is significantly influenced by the ASE noise. Therefore, it is necessary to adequately discuss fluctuations of the intensity and the resulting photoelectron statistics in theoretical analyses of soliton communication systems.

The ASE light amplitude can be generally considered to have Gaussian statistics. As has been investigated previously [2, 3], fluctuations of photoelectron counts differ from the Gaussian random process when a deterministic signal is superposed with the Gaussian light. However, the derivation of the exact PDF has been neglected in studies on on-off keying communication systems (including those using soliton pulses) because of its complication and approximations with the Gaussian or the Laguerre PDF have been used in previous works [1, 4]. Recently Tang and Ye [5] have calculated bit error rates of soliton communication systems by using a noncentral χ^2 PDF, which is an approximated PDF for the integrated intensity and is related to the Laguerre PDF by the inverse Poisson transform.

In this paper we present the results of a theoretical investigation on the PDF of photoelectron counts when a signal having a pulse shape similar to a fundamental soliton is detected together with the ASE light. The analysis is conceptually simple. Complications arise only from the necessity of computing a characteristic function. The PDF presented herein has the following features: (i) The use of general theory [2, 3] makes it possible to find the exact PDF, (ii) the effects of the soliton pulse profile and its width are taken into account, and (iii) the optical filter is assumed to have a Lorentzian passband, a realistic profile for commonly used Fabry-Pérot filters.

After a brief review of the general formalism, the PDF for the integrated intensity is calculated in Sec. II by expanding the mixed amplitude in terms of orthogonal basis functions. From this PDF, we obtain the PDF for photoelectron counts in Sec. III. Results are applied in Sec. IV to a receiver equipped with an optical preamplifier and differences from the Gaussian PDF are discussed. In order to show the differences clearly, the skewness and the kurtosis are utilized as measures. In addition, the accuracy of the Laguerre approximation is also evaluated. Although this paper discusses an optical preamplifier in detail, we can readily apply the analysis to any configuration of the cascaded chain of optical amplifiers. The purpose of this paper is to show the influence of the interferential beating upon the PDF and thus other major effects degrading bit error rates, such as timing jitter (the Gordon-Haus effect [6]) and the receiver thermal noise, are left out of the analysis.

II. INTEGRATED INTENSITY

A. Orthogonal expansion

In this subsection the technique of expanding the integrated intensity in terms of an orthogonal basis is reviewed for a deterministic signal mixed with chaotic light [2, 3]. The integrated intensity is defined as

1050-2947/95/51(2)/1662(7)/$06.00

$$W = \int_0^T |V(t)|^2 dt \ , \tag{1}$$

where T is the counting interval and $V(t)$ is the complex amplitude of the detected optical field normalized such that the instantaneous intensity $|V(t)|^2$ has the unit of photon arrival rate (photon/second). We consider the superposition of a deterministic signal of the optical frequency ν_0 and linearly polarized chaotic light whose power spectrum is centered at ν_0. The complex amplitude of this mixed field can be written as

$$V(t) = V_s(t) + V_t(t) \ , \tag{2}$$

where the subscripts s and t indicate the signal and the chaotic light, respectively. $V_t(t)$ is assumed to be a stationary complex Gaussian random process with zero mean.

The Karhunen-Loève theorem allows $V_t(t)$ to be expanded into an orthogonal basis with coefficients uncorrelated over the interval $(0, T)$ [3, 7–9]. The mixed amplitude $V(t)$ can also be formally expanded in terms of this basis as [2, 3]

$$V(t) = \sum_{k=0}^{\infty} \sqrt{T}(a_{sk} + a_{tk})\phi_k(t) \quad (0 \le t \le T) \ , \tag{3}$$

$$a_{sk} = \frac{1}{\sqrt{T}} \int_0^T V_s(t)\phi_k^*(t)dt \ , \tag{4}$$

$$a_{tk} = \frac{1}{\sqrt{T}} \int_0^T V_t(t)\phi_k^*(t)dt \ , \tag{5}$$

where the subscript k indicates the kth mode component. The coefficients of the chaotic part a_{tk} are statistically uncorrelated complex Gaussian variables and the basis $\phi_k(t)$ is orthogonal over the interval $0 \le t \le T$, i.e.,

$$\int_0^T \phi_j(t)\phi_k^*(t)dt = \delta_{jk}. \tag{6}$$

Upon substituting (3) into (1), we can rewrite W as the sum of contributions of all modes

$$W = \sum_{k=0}^{\infty} T|a_{sk} + a_{tk}|^2 = \sum_{k=0}^{\infty} W_k \ , \tag{7}$$

where

$$W_k = W_{sk} + W_{tk} + 2T\mathrm{Re}[a_{sk}a_{tk}^*], \tag{8}$$

$W_{sk} = |a_{sk}|^2 T$, and $W_{tk} = |a_{tk}|^2 T$. The last term of (8) represents fluctuations due to interference of the kth mode components. The basis $\phi_k(t)$ and variance of a_{tk} can be determined by solving the integral equation [2, 3, 7–14]

$$\int_0^T R(t-\tau)\phi_k(\tau)d\tau = \sigma_{tk}^2 T\phi_k(t) \ , \tag{9}$$

where $R(\ )$ is the autocorrelation function of $V_t(t)$ and $\sigma_{tk}^2 = \langle |a_{tk}|^2 \rangle$ is the variance of a_{tk}. If we assume that $|V_t(t)|$ has the variance σ_t^2 [$= R(0)$] with a Lorentzian power spectrum of bandwidth[1] B_0, $R(\tau)$ takes the form

$$R(\tau) = \sigma_t^2 e^{-B_0|\tau|}. \tag{10}$$

Here the variance σ_t^2 is related to the average integrated intensity of the chaotic light by $\langle W_t \rangle = \sigma_t^2 T$. In several papers [2, 3, 7–11] the integral equation (9) has been solved for this $R(\tau)$ with the result

$$\langle W_{tk} \rangle = \langle W_t \rangle \frac{2\beta}{\beta^2 + (\omega_k T)^2} \ , \tag{11}$$

where $\beta = B_0 T$, $\langle W_t \rangle = \sum_k W_{tk}$, and ω_k is a positive root of either of the following two equations:[2]

$$\omega_k T \tan\frac{\omega_k T}{2} = \beta \ , \tag{12}$$

$$\omega_k T \cot\frac{\omega_k T}{2} = -\beta. \tag{13}$$

The basis corresponding to $\omega_k T$ given by (12) is

$$\phi_k(t) = \sqrt{\frac{2}{T(1 + \langle W_{tk} \rangle / \langle W_t \rangle)}} \cos\left[\omega_k T\left(\frac{t}{T} - \frac{1}{2}\right)\right]. \tag{14}$$

Replacing cos( ) in (14) by sin( ) yields immediately the expression of ϕ_k related to (13).

B. Probability density function

Since the sum of a complex constant and a complex Gaussian variable is generally a complex Gaussian variable, $a_{sk} + a_{tk}$ in (7) is a complex Gaussian variable, whose real and imaginary parts have equal variances. The PDF for W_k ($= T|a_{sk} + a_{tk}|^2$) is thus the Bessel PDF, with the result that its characteristic function is [2, 3]

$$\Phi_{Wk}(u) = \langle e^{iuW_k} \rangle = \frac{1}{1 - iu\langle W_{tk} \rangle} \exp\left(\frac{iuW_{sk}}{1 - iu\langle W_{tk} \rangle}\right). \tag{15}$$

If the deterministic signal is assumed to have a pulse shape similar to a fundamental soliton centered at the time t_0, $V_s(t)$ is expressed as [16]

$$V_s(t) = \sqrt{\frac{P_s}{h\nu_0}} \mathrm{sech}\left(\frac{t - t_0}{T_0/2}\right) \ , \tag{16}$$

where P_s is the peak power on a detector, T_0 is a pulse full width at $1/e$ power point, and h is Planck's constant. By substituting (14) and (16) into (4) and using the defini-

[1]The linewidth B_0 is defined as the linewidth that have been introduced by Mandel and Wolf [15]. For the Lorentzian power spectrum, we can find the relation $B_0 = \pi B_L$, where B_L is the full width at half maximum point (FWHM).

[2]We assume that the ω_k are arranged so that $\omega_0 < \omega_1 < \omega_2 < \cdots$.

tion $W_{sk} = |a_{sk}|^2 T$, we can calculate W_{sk}, which is simplified when the soliton lies at the center of T ($t_0 = T/2$) and has a sufficiently narrow width ($T_0 \ll T$) such that most of the energy is contained within the interval T. For $\omega_k T$ related to (12), the result is

$$W_{sk} = \frac{\pi^2 W_s/(T/T_0)}{2(1+\langle W_{tk}\rangle/\langle W_t\rangle)} \mathrm{sech}^2\left(\frac{\pi\omega_k T}{4(T/T_0)}\right) , \quad (17)$$

where W_s ($= P_s T_0/h\nu_0 = \sum_k W_{sk}$) is the integrated intensity of the soliton. For $\omega_k T$ determined from (13), $W_{sk} = 0$ since sin( ) in $\phi_k(t)$ is an odd function with respect to the center of T.

Since uncorrelated Gaussian variables are, in general, also statistically independent [17], a_{tk} and the resulting W_k are independent variables. The characteristic function of W is therefore given by the infinite products of (15):

$$\Phi_W(u) = \prod_{k=0}^{\infty} \frac{1}{1-iu\langle W_{tk}\rangle} \exp\left(\sum_{k=0}^{\infty} \frac{iuW_{sk}}{1-iu\langle W_{tk}\rangle}\right). \quad (18)$$

By taking the Fourier transform, we obtain the result

$$f_W(W) = \frac{1}{2\pi}\int_{-\infty}^{\infty}\left[\cosh y_W + \frac{1}{2}\left(\frac{\beta}{y_W}+\frac{y_W}{\beta}\right)\sinh y_W\right]^{-1} \times\exp\left[-iuW+\beta+\sum_{k=0}^{\infty}\frac{iuW_{sk}}{1-iu\langle W_{tk}\rangle}\right]du , \quad (19)$$

where $y_W^2 = \beta^2 - 2(iu)\beta\langle W_t\rangle$ and we made use of a closed form of $\Phi_W(u)$ given for the case when only the chaotic light is present ($W_{sk} = 0$) [3, 9, 11, 14]. In the case of a signal alone without chaotic light ($W_{tk} = 0$), the δ function $\delta(W - W_s)$ is obtained.

By using their definition [18] the cumulants associated with (18) can be obtained as

$$(\kappa_m)_W = \sum_{k=0}^{\infty}\left[(m-1)!\langle W_{tk}\rangle + m! W_{sk}\right]\langle W_{tk}\rangle^{m-1}. \quad (20)$$

For $m = 1$ and 2, Eq. (20) directly yields the average and variance of W, respectively,

$$\langle W\rangle = W_s + \langle W_t\rangle , \quad (21)$$

$$\sigma_W^2 = (\sigma_W^2)_t + \frac{2W_s\langle W_t\rangle}{TT_0}\iint_0^T \mathrm{sech}\left(\frac{t_1-t_0}{T_0/2}\right) \times\mathrm{sech}\left(\frac{t_2-t_0}{T_0/2}\right) e^{-B_0|t_1-t_2|}dt_1 dt_2 , \quad (22)$$

where

$$(\sigma_W^2)_t = \sum_{k=0}^{\infty}\langle W_{tk}\rangle^2 = \frac{\langle W_t\rangle^2(e^{-2\beta}+2\beta-1)}{2\beta^2} \quad (23)$$

is the variance in the absence of the signal ($W_s = 0$) [3, 9, 11], and we used the relation

$$R(t_1-t_2) = \sum_{k=0}^{\infty}\langle W_{tk}\rangle\phi_k(t_1)\phi_k^*(t_2). \quad (24)$$

The first and second terms in (22) arise from beating the chaotic light against itself and against the soliton, respectively.

III. PHOTOELECTRON COUNTS

We consider photoelectric detection with a small area detector having the quantum efficiency η. Photoelectron statistics can be completely described by the statistical properties of the integrated intensity. The PDFs for the photoelectron count n and for the integrated intensity W are related by the well-known Poisson transformation [3, 19]. In the corresponding characteristic functions, it is necessary only to replace iu by $\eta(e^{iu}-1)$. Thus, we have

$$f_n(n) = \frac{1}{2\pi}\int_{-\infty}^{\infty}\left[\cosh y_n + \frac{1}{2}\left(\frac{\beta}{y_n}+\frac{y_n}{\beta}\right)\sinh y_n\right]^{-1} \times\exp\left[-iun+\beta +\sum_{k=0}^{\infty}\frac{\eta W_{sk}(e^{iu}-1)}{1-\eta\langle W_{tk}\rangle(e^{iu}-1)}\right]du , \quad (25)$$

where $y_n^2 = \beta^2 - 2\eta\beta\langle W_t\rangle(e^{iu}-1)$. A closed form of $f_n(n)$ is difficult to obtain, but the integral in (25) is easy to perform numerically. In the absence of the chaotic light, $f_n(n)$ in (25) becomes the Poisson PDF having the average ηW_s.

Low-order cumulants of $f_n(n)$ can be readily related to those of $f_W(W)$ by [3, 19]

$$\begin{aligned}(\kappa_1)_n &= \eta(\kappa_1)_W ,\\ (\kappa_2)_n &= \eta^2(\kappa_2)_W + \eta(\kappa_1)_W ,\\ (\kappa_3)_n &= \eta^3(\kappa_3)_W + 3\eta^2(\kappa_2)_W + \eta(\kappa_1)_W ,\\ (\kappa_4)_n &= \eta^4(\kappa_4)_W + 6\eta^3(\kappa_3)_W + 7\eta^2(\kappa_2)_W + \eta(\kappa_1)_W.\end{aligned} \quad (26)$$

The average and the variance are then given by

$$\langle n\rangle = \eta(W_s + \langle W_t\rangle) , \quad (27)$$

$$\sigma_n^2 = \langle n\rangle + \eta^2\sigma_W^2. \quad (28)$$

The first term of the variance originates from the shot noise of the soliton and the chaotic light, whereas the second term is the contribution of intensity fluctuations due to the beating of the soliton and the chaotic light.

IV. STATISTICS OF AMPLIFIED PULSES

A. Exact PDF and the Gaussian approximation

The partition coefficient of the average integrated intensity for chaotic light $\langle W_{tk}\rangle/\langle W_t\rangle$, which measures the fraction of mode energy and is obtained from (11) with (12) or (13), is plotted in Fig. 1 as a function of the mode index k. Figure 2 shows the same quantity for a signal W_{sk}/W_s obtained from (17) using the data plotted in

Fig. 1. We note that $W_{sk}/W_s = 0$ when k is odd and that the sum over all k is unity. As can be readily understood from the fact that the Karhunen-Loève expansion is a kind of extended Fourier series, the energy of the chaotic light is distributed over a wide range of k, while that of the signal is centered on low modes because of its deterministic nature. By calculating the PDF (25) based on these plots, we can take into account contributions of the spectral profile of the chaotic light as well as of the signal pulse profile. Since W_{sk} and $\langle W_{tk}\rangle$ appearing in (25) are calculated from W_s and $\langle W_t\rangle$ for given β and T/T_0, our analysis can be applied to any type of the cascaded chain of amplifiers if we use proper values of W_s and $\langle W_t\rangle$ (see the appendix).

As an example of practical application, we consider a configuration in which a launched fundamental soliton is detected after experiencing loss along the fiber link and being amplified by an optical preamplifier equipped with a Lorentzian bandpass (optical) filter. The amplitude of the filtered ASE field may be regarded as a complex Gaussian random variable with zero mean.

In this case, the integrated intensity of the signal at the detector is given by

$$W_s = GP_{s0}T_0/h\nu \ , \tag{29}$$

where P_{s0} is the optical peak power of the signal at the amplifier input and G is the power gain. At the optical filter input, the average integrated intensity of the ASE light on each mode is nearly constant and is given by [1, 20]

$$\langle W_{tk}\rangle = (G-1)\rho \ , \tag{30}$$

where ρ is the spontaneous-emission factor of the amplifier. Equating (30) and the relation

$$\langle W_{tk}\rangle = (2/\beta)\langle W_t\rangle, \tag{31}$$

which is obtained from (11) for $\omega_k T \ll \beta$ (corresponding to low frequencies in the Fourier series), we obtain the

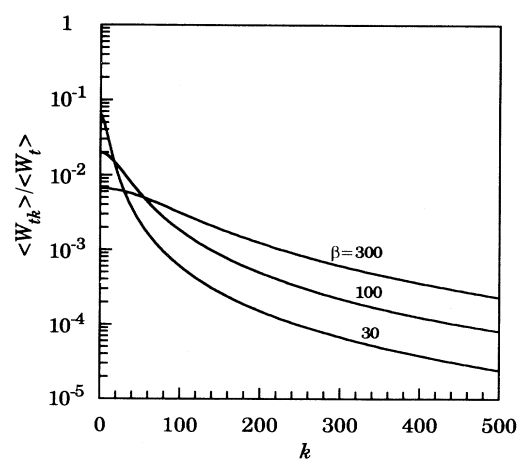

FIG. 1. Partition coefficient of the average integrated intensity for chaotic light plotted as a function of the mode index k.

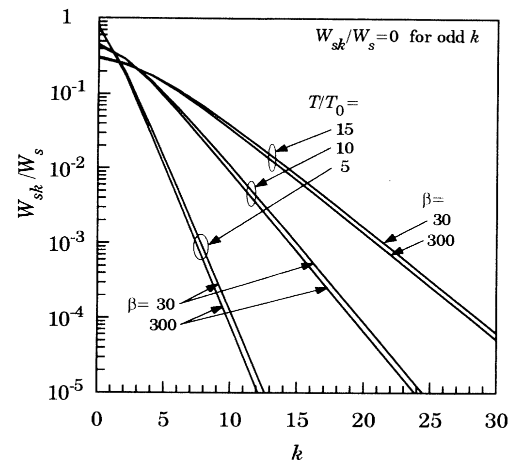

FIG. 2. Partition coefficient of the integrated intensity for a signal associated with a soliton plotted as a function of the mode index k.

total amount of the ASE reaching the detector as

$$\langle W_t\rangle = (G-1)\rho(\beta/2). \tag{32}$$

The quantity $\beta/2$ expresses the product of T and the (equivalent) noise bandwidth [17] of the Lorentzian optical filter $B_0/2$. The mean and the variance of n are then given by

$$\langle n\rangle = \eta\left(\frac{GP_{s0}}{h\nu_0} + \frac{(G-1)\rho\beta}{2}\right) , \tag{33}$$

$$\sigma_n^2 = \langle n\rangle + (\sigma_n^2)_t + (\sigma_n^2)_{s-t} \ , \tag{34}$$

$$(\sigma_n^2)_t = \frac{1}{4}\left[\eta\rho(G-1)\right]^2 (e^{-2\beta} + 2\beta - 1) \ ,$$

$$(\sigma_n^2)_{s-t} = \frac{\eta^2\rho\beta G(G-1)P_{s0}}{h\nu_0 T} \times \iint_0^T \operatorname{sech}\left(\frac{t_1 - t_0}{T_0/2}\right) \operatorname{sech}\left(\frac{t_2 - t_0}{T_0/2}\right) \times e^{-B_0|t_1-t_2|}dt_1 dt_2.$$

The signal-to-noise power ratio[3] of n is computed from $S/N = (\eta W_s)^2/\sigma_n^2$ as a function of β and is plotted in Fig. 3. Typical parameter values for the optical preamplifier and receiver were used for the computation. The received peak power before amplification was chosen such that the optical power averaged over T was -40 dBm. It is obvious from Fig. 3 that S/N degrades, or decreases, with increasing β and is influenced considerably by the pulse width T_0 when β is small.

Figures 4 and 5 show the exact PDFs calculated for n with β and T/T_0 as parameters, respectively. The curves were obtained by using (25) together with the data plotted in Figs. 1 and 2 and the fast-Fourier-transform tech-

[3]The signal and the noise power represent the power of the random process n. Therefore, S is defined as the square of the signal part in (33) and N is given by (34).

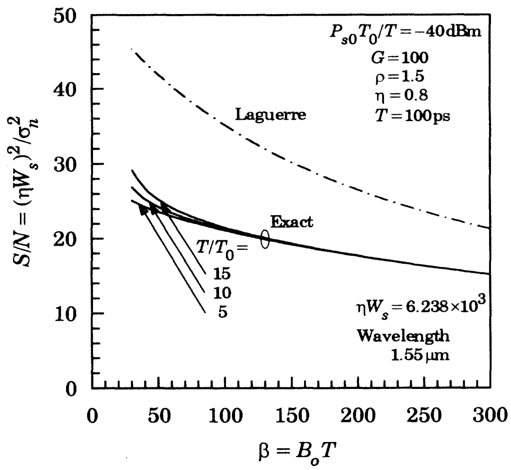

FIG. 3. Signal-to-noise power ratio of photoelectron counts n.

nique. The parameters used for the computation are the same as in Fig. 3. For a specific value T=100 ps corresponding to a bit rate of 10 Gbit/s, β =30, 100, and 300 correspond to the bandwidths (FWHM) B_L =95.5, 318, and 955 GHz, respectively. Also shown are the Gaussian PDFs, each of which has the same variance as the corresponding exact one. Although not shown, the normalized PDF of W would be nearly the same as that of n because contributions from shot noise, or the first term in (28), are negligible when such a strong signal is incident on the detector. Peaks on the exact curves are indicated in the figures. Clearly the exact PDFs are not symmetric around the mean $n/\langle n\rangle = 1$ and their peaks deviate toward the left side of the mean. The exact PDFs thus form a short tail on the left side of the mean and a long tail on the other side. In addition, the peaks are somewhat taller than those of the Gaussian PDFs. A comparison of the exact and Gaussian PDFs shows clearly that, although the variances are equal, the left tail of the

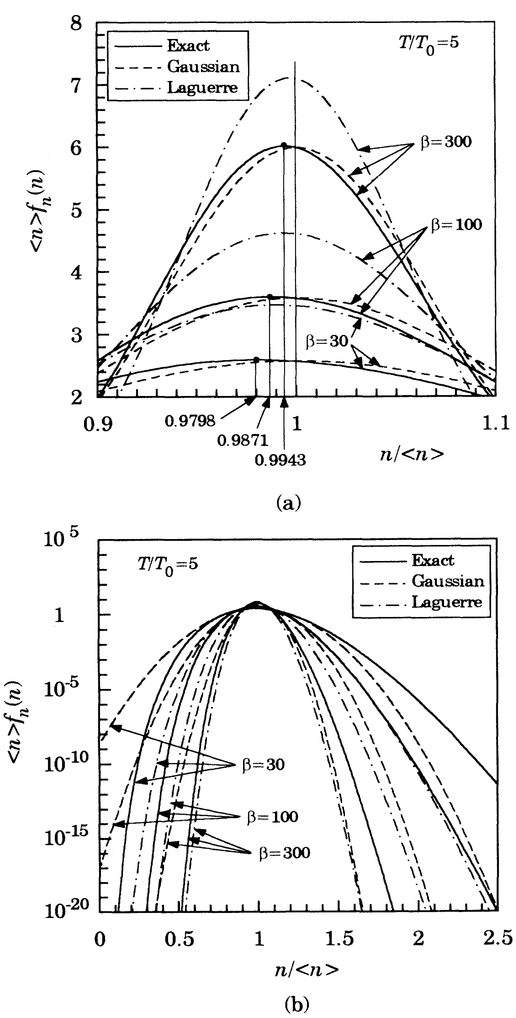

FIG. 4. Probability density function for photoelectron counts plotted for $T/T_0 = 5$. (a) Plots in the neighborhood of the mean. (b) Logarithm scale.

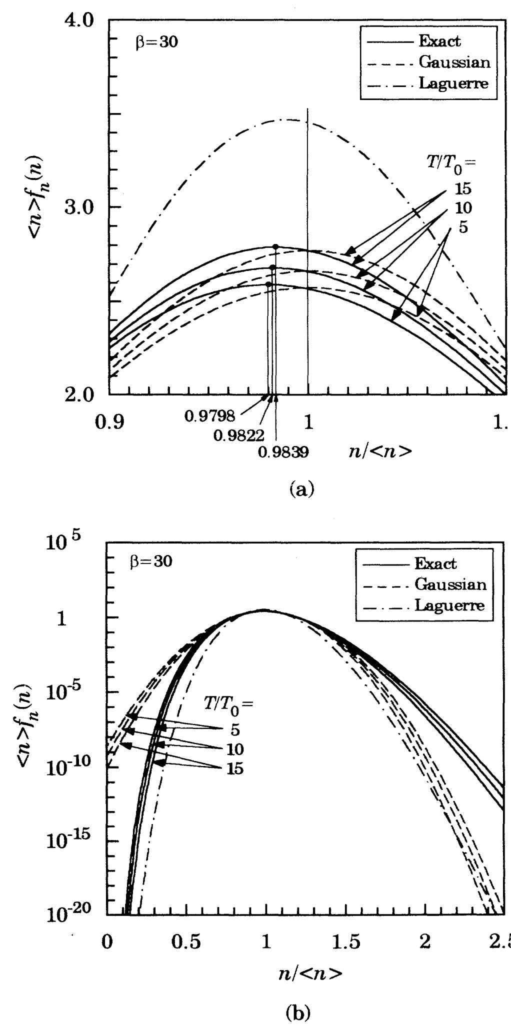

FIG. 5. Probability density function for photoelectron counts plotted for β = 30. (a) Plots in the neighborhood of the mean. (b) Logarithm scale.

PDF is overestimated if the Gaussian approximation is used. In Figs. 4 and 5 the Gaussian approximation overestimates the PDF by many orders of magnitude in the left tail near $\langle n\rangle f_n(n) \sim 10^{-12}$, a region that is used to calculate the bit error rates $\sim 10^{-11}$ in soliton communication systems. Therefore, the use of a Gaussian PDF approximation is likely to overestimate the bit error rate considerably.

As useful measures to represent differences between the Gaussian PDF and the exact PDF, we introduce the skewness γ_1 and the kurtosis (excess) γ_2, defined by [18]

$$\gamma_1 = \frac{(\kappa_3)_n}{\sigma_n^3}, \quad \gamma_2 = \frac{(\kappa_4)_n}{\sigma_n^4}. \tag{35}$$

Both of these quantities are exactly zero for a Gaussian PDF. In Fig. 6, γ_1 and γ_2 of the exact PDFs are shown. As can be readily expected from Figs. 4 and 5, γ_1 and γ_2 take positive values. With increasing β, the skewness and kurtosis decrease, i.e., the PDF approaches the Gaussian PDF according to the central limit theorem because a large number of modes contribute (see Fig. 1) and the number of terms in (18) increases. Although γ_1 and γ_2 decrease with T/T_0, Fig. 6 shows that both are hardly affected by T/T_0 for large β.

B. Laguerre approximation

If the filtered ASE light is assumed to excite a large number of modes ($M \gg 1$) uniformly (corresponding to a rectangular function in Fig. 1), the PDF for its mixture with a deterministic signal can be given by the Laguerre PDF [20]

$$f_n(n) = \frac{(\eta p)^n}{(1+\eta p)^{n+M}} \exp\left(-\frac{\eta W_s}{1+\eta p}\right) \times L_n^{M-1}\left(-\frac{\eta W_s}{(1+\eta p)\eta p}\right), \tag{36}$$

$$\langle n\rangle = \eta(W_s + \langle W_t\rangle),$$
$$\sigma_n^2 = \langle n\rangle + \eta^2(\langle W_t\rangle^2 + 2W_s\langle W_t\rangle)/M, \tag{37}$$

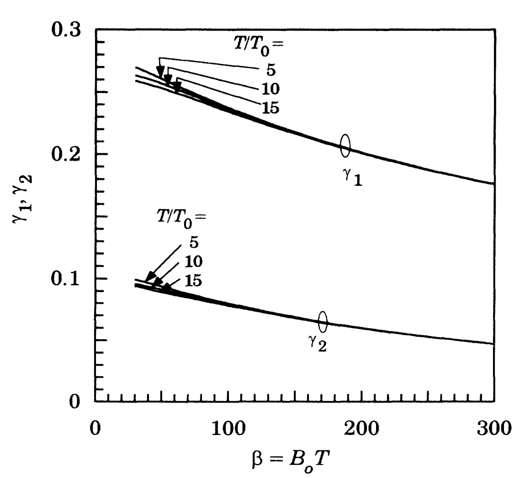

FIG. 6. Skewness γ_1 and kurtosis γ_2 of the exact probability density function.

where $p = \langle W_t\rangle/M$ and $L_n^m(\ )$ are the Laguerre polynomials. Through several approaches [4, 21], the Laguerre PDF has been derived for a signal with a constant amplitude over T. The corresponding PDF for W is the non-central χ^2 PDF, which has been recently applied to the bit error rate calculation in soliton communication systems [5]. The parameter M has been taken to be $\beta = B_0T$ in previous work[4] [5].

The Laguerre PDF is determined only from $\langle W_t\rangle$, W_s and M; hence it is independent of the received pulse profile. In Figs. 3–5, we plot its signal-to-noise ratio and PDF. A comparison with the exact curves indicates that the Laguerre approximation underestimates the variance (or the noise power) and that, in the case of Figs. 4 and 5, the left side tail is underestimated by many orders of magnitude in the tail of the PDF where $\langle n\rangle f_n(n) \sim 10^{-12}$. This is because our analysis has included the effect of a Lorentzian bandpass optical filter and the soliton pulse profile. We should note that the Lorentzian PDF corresponds to a rectangular spectrum in place of a Lorentzian. The errors associated with the Laguerre PDF are attributed mainly to differences in the variances, especially the terms representing the beating of the signal against spontaneous emission, or $(\sigma_n^2)^2_{s-t}$ in (34) and the last term of σ_n^2 in (37). As a result, if bit error rates of the soliton communication systems employing Lorentzian filters are calculated by using the Laguerre PDF, they will be lower than the actual values for a given decision (threshold) level.

V. CONCLUSIONS

We have investigated the PDF and its approximations for photoelectron counts of a soliton signal mixed with filtered ASE light. Based on an expansion of the field amplitude in terms of an orthogonal basis, we have obtained the exact PDF and applied it to a receiver equipped with a Lorentzian optical bandpass filter. The theoretical analysis includes not only the effects of the bandpass filter but also of the soliton pulse shape. We have found that photoelectron statistics is influenced considerably by both the shape associated with a soliton and the pulse width when the product B_0T of the optical bandwidth and counting interval is small. However, the effects of the pulse width become negligible for large values of B_0T. Using the skewness and the kurtosis as judging criteria, the differences between the exact PDF and its Gaussian approximation have been quantified. In addition, we have evaluated the accuracy of the Laguerre approximation that is widely used for bit error rate calculations. Our results indicate that the use of both the Gaussian and the Laguerre PDF leads to considerable errors. The bit error rate is overestimated by several orders of magnitude for the Gaussian PDF, while it is underes-

[4]When the Laguerre PDF is applied to the Lorentzian ASE spectrum, it is necessary to compensate for approximation errors by adjusting M in an appropriate way [22].

timated by a large amount for the Laguerre PDF. The results of this paper should prove useful when an accurate estimate of the bit error rates of soliton communication systems is required.

ACKNOWLEDGMENT

The work is supported in part by the U.S. Army Research Office under the University Research Initiative Program.

APPENDIX: CASCADED AMPLIFIERS

For a cascaded chain of N amplifiers, the integrated intensity of a signal at the detector is given by

$$W_s = L_e P_s T_0 / h\nu \ , \tag{A1}$$

where P_s is the soliton peak power at the transmitter output. $L_e = L_1 G_1 \cdots L_N G_N L_{N+1}$ is the effective net loss of the fiber link. Here G_j is the power gain of the jth amplifier and L_j is the loss between $j-1$ and jth amplifiers. L_1 and L_{N+1} are the losses between the transmitter and the first amplifier and between the last amplifier and detector, respectively. The integrated intensity of the ASE field at the detector is obtained as the sum of contributions of each amplifier. Because such contributions are statistically independent, it can be written as

$$\langle W_t \rangle = K\rho(\beta/2) \ , \tag{A2}$$

where

$$K = L_e \left(\frac{G_1 - 1}{G_1 L_1} + \frac{G_2 - 1}{G_1 L_1 G_2 L_2} + \cdots + \frac{G_N - 1}{G_1 L_1 \cdots G_N L_N} \right) . \tag{A3}$$

By using (A1) and (A2) instead of (29) and (32), we can apply our theory to any configuration of the cascaded chain of amplifiers. If $N = 1$, the configuration $L_e = L_1 G_1 L_2$ corresponds to an in-line amplifier, becomes a preamplifier for $L_2 = 1$, and a postamplifier for $L_1 = 1$.

When $G_1 L_1 = \cdots = G_N L_N = 1$ and $L_{N+1} = 1$, the configuration corresponds to a loss-compensated fiber link with amplifiers. Furthermore, it approaches a continuous distributed amplifier (or active line) for a given loss between the transmitter and the receiver as $N \to \infty$.

[1] G. P. Agrawal, *Fiber-Optic Communication Systems* (Wiley, New York, 1992).
[2] E. Jakeman and E. R. Pike, J. Phys. A **2**, 115, 1969.
[3] B. Saleh, *Photoelectron Statistics* (Springer-Verlag, Berlin, 1978), pp. 206–213.
[4] T. Li and M. C. Teich, Electron. Lett. **27**, 598 (1991).
[5] X. Tang and P. Ye, Opt. Lett. **18**, 1156 (1993).
[6] J. P. Gordon and H. A. Haus, Opt. Lett. **11**, 665 (1986).
[7] W. B. Davenport and W. L. Root, *An Introduction to the Theory of Random Signal and Noise* (McGraw-Hill, New York, 1958).
[8] D. Slepian, Bell Syst. Tech. J. **37**, 163 (1958).
[9] E. Jakeman and E. R. Pike, J. Phys. A **1**, 128 (1968).
[10] D. Slepian, Trans. IRE **3**, 68 (1954).
[11] A. K. Jaiswal and C. L. Mehta, Phys. Rev. **186**, 1355 (1969).
[12] A. K. Jaiswal and C. L. Mehta, Phys. Rev. A **2**, 168 (1970).
[13] C. W. Helstrom, Proc. Phys. Soc. London **83**, 777 (1964).
[14] G. Bédard, Phys. Rev. **151**, 1038 (1966).
[15] L. Mandel and E. Wolf, Proc. Phys. Soc. London **80**, 894 (1962).
[16] G. P. Agrawal, *Nonlinear Fiber Optics* (Academic, San Diego, 1989).
[17] P. Z. Peebles, *Probability, Random Variables, and Random Signal Principles*, 2nd ed. (McGraw-Hill, New York, 1987).
[18] H. Cramér, *Mathematical Methods of Statistics* (Princeton University Press, Princeton, 1946).
[19] L. Mandel, in *Progress in Optics*, edited by E. Wolf (North-Holland, Amsterdam, 1963), Vol. 2, pp. 181–248.
[20] H. A. Steinberg, Proc. IEEE, **52**, 28 (1964).
[21] J. Peřina, Phys. Lett. **24A**, 333 (1967).
[22] R. Horák, L. Mišta, and J. Peřina, J. Phys. **4**, 231 (1971).